

Pitting Corrosion Behavior of UNS S31803 and UNS S32304 Duplex Stainless Steels in 3.5 wt% NaCl Solution

José Carlos de Lacerda¹, Ricardo Luiz Perez Teixeira¹,
Rafaela Maria Ribeiro de Souza¹, Renata Braga Soares²,
Vanessa de Freitas Cunha Lins²

¹Mechanical and Materials Engineering, Universidade Federal de Itajubá, Itabira Campus MG, Brazil, 35903-087.

e-mail: jlacerda@unifei.edu.br, ricardo.luiz@unifei.edu.br, rafarib4@gmail.com, valdirsignoretti@unifei.edu.br

²Chemical Engineering Department, Universidade Federal de Minas Gerais, Belo Horizonte MG, Brazil, 31270-901.

e-mail: renatabragasoares@yahoo.com.br, vlins@deq.ufmg.br

ABSTRACT

This work examined the pitting corrosion resistance of two types of duplex stainless steels: UNS S31803, with molybdenum, and UNS S32304, without molybdenum. Cyclic potentiodynamic polarization and critical pitting temperature (CPT) tests were performed in 3.5 wt% NaCl solution. Scanning electron microscopy (SEM) was used for analysis of the pits on the surface of samples. The two steels studied presented susceptible to pitting corrosion in 3.5 wt% NaCl solution. UNS S31803 steel showed a higher corrosion potential (E_{corr}), pitting potential (E_{pit}), and polarization resistance (R_p) compared to UNS S32304 steel. It was also observed that the UNS S31803 steel showed higher capacity to repassivation and CPT than the UNS S32304 steel.

Keywords: Duplex stainless steels; Pitting potential; Electrochemical impedance spectroscopy; Cyclic potentiodynamic polarization; CPT.

1. INTRODUCTION

Pitting corrosion is a highly localized form of corrosion attack and it is characterized for presenting a very small attacked area compared to the total area exposed to the corrosive environment [1]. This type of corrosion occurs in stainless steels in most cases in the presence of environments containing chlorides or when there is incomplete passivation [2]. Pitting corrosion results from the breakdown of the passive layer of stainless steel, motivated by metallurgical characteristics such as inclusions, grain boundary, or intermetallic constituents [3]. The breaking of the passive layer results in the formation of an electrochemical cell, where the anode is the active area and the cathode is the passive area.

This type of corrosion is typical of metals/alloys that form a thin protective film of oxide or hydroxide of about 30 to 80 Å of thickness, called the passive layer. Some examples of materials that form this passive layer are stainless steels, aluminum, nickel, chromium, and others [4]. When unbroken, the passive film significantly reduces the contact between the electrolyte and the metal (anode). Thus, the density of the anodic current becomes practically a constant value of about 1 $\mu\text{A}/\text{cm}^2$. This amounts to saying that the material may corrode, but at a negligible rate. However, when the protective film breaks, it forms an electrochemical cell consisting of the anode, a small metal area exposed by the rupture of the film, and the cathode, the largest area protected by the film. The potential difference between these regions causes a flow of high current, with rapid corrosion of the anode area. Once the formation of the pit is initiated, it will continue as a self-catalytic process.

The duplex stainless steel is a steel that has a biphasic microstructure composed of ferrite and austenite in volume ratio of approximately 50% each of the phases. UNS S32304 steel is considered low alloy among the duplex stainless steels due to its lower proportion of alloying elements, thus providing lower cost. UNS S31803 steel is considered middle alloy, with a greater range of use, with the emphasis on the presence of molybdenum in its composition [5, 6].

Duplex stainless steels are characterized by the combination of high corrosion resistance and high mechanical strength. Therefore, the duplex stainless steels have been chosen for applications in the chemical and petrochemical industry, reactors, heat exchangers, pipelines, nuclear power plants, and pulp and paper mills. The high corrosion resistance of those steels is due to the formation of the thin passive layer of

chromium/iron oxide strongly adhered on the surface [7-9]. The breaking of the passive layer exposes the steel to the formation of pitting corrosion. Duplex stainless steels are susceptible to this type of corrosion when exposed to an environment containing chlorides [10].

The presence of chromium, molybdenum, and nitrogen as alloying elements in stainless steels increases their resistance to pitting corrosion. In the case of duplex stainless steels UNS S31803 and UNS S32304, the most important difference in their chemical composition is the molybdenum present in the former one [7,11,12]. Other factors that can influence the formation of pits in stainless steel include temperature, cleaning and surface finish, microstructure, defects, environment, and applied potential.

The susceptibility to pitting formation increases with temperature. The influence of temperature on pitting formation can be indicated by the critical pitting temperature (CPT) of steel. CPT is the lowest temperature at which stable pit formation begins. The environment containing chlorides destabilizes the passive layer affecting the resistance to pitting corrosion. Regarding the surface finish, the more uniform the polished surface of the sample, the greater the pitting resistance [7, 12, 13].

This work aims to assess the pitting corrosion resistance and the repassivation potential of stainless steels UNS S31803 (containing molybdenum) and UNS S22304 (without molybdenum) by electrochemical impedance spectroscopy, cyclic polarization, and CPT tests.

2. MATERIALS AND METHODS

Duplex stainless steel plates type UNS S31803 and UNS S32304, cold rolled and annealed at 1060°C, were used for the tests. The plates of stainless steel were supplied by APERAM South America, Brazil. Table 1 shows the chemical composition of the steels, obtained using a CS-400 carbon analyzer and ARL 4460 optical emission spectrometer.

Table 1: Chemical composition of UNS S31803 and UNS S32304 steels.

ELEMENT (wt%)	C	Si	Mn	Cr	Ni	Mo	N
UNS S32304	0.03	0.41	1.56	23.01	4.51	0.31	0.13
UNS S31803	0.02	0.31	1.82	22.38	5.35	3.04	0.15

A potentiostat EmStat 3 (Palm Sens) was used for the potentiodynamic polarization tests. The potentials were performed from $-0.5 V_{SCE}$ to $1.6 V_{SCE}$ at a scanning rate of $0.167 mV_{SCE}/s$. An electrochemical cell containing three electrodes was used: the reference electrode saturated calomel (SCE), the counter platinum electrode, and the working electrode (specimen). The tests were performed at 25°C. Three tests were performed in each of the steels.

The specimens were prepared from a $1 cm^2$ section of the UNS S31803 and UNS S32304 steel sheets, and they were welded to a wire (for electrical contact) and embedded in polyester resin. Before each electrochemical measurement, the electrode surface was subjected to a standard procedure to remove any corrosion layer formed and to remove surface irregularities. The samples were polished with SiC paper with grain size of 240, 320, 400, and 600 grit, respectively, according to ASTM G5-14e1 [14]. After polishing, the specimens were rinsed with deionized water and 70% ethanol v/v, and dried with a hot air jet. A relaxation time of 1 h was performed to stabilize the stainless steel samples at OCP before potentiodynamic polarization test.

Multiple electrochemical impedance spectroscopy (EIS) scans by inductive loop at low-frequency mode and cyclic polarization tests were performed using an AUTOLAB PGSTAT 302N potentiostat/galvanostat, and NOVA 1.11 software. Electrochemical measurements were performed at room temperature using an electrochemical cell with a capacity of 200 mL and three electrodes: the working electrode, a platinum counter electrode, and a silver/silver chloride as the reference electrode. The

electrolytic solution used was 3.5 wt% NaCl solution. The exposed area of duplex steel samples in contact with the electrolyte was 1cm². The working electrode was the UNS S31803 and UNS S32304 steels.

Electrochemical tests were preceded by immersing the samples in the test solution for 3600 seconds to stabilize the open circuit potential. After measuring the open circuit potential, the duplex steel samples were analyzed using the technique of electrochemical impedance spectroscopy in the frequency range from 10 kHz to 10 mHz and a potential amplitude of 10 mV with respect to the open circuit potential. The ZviewTM software was used for simulation of the equivalent circuit. Impedance measurements were performed in triplicate. Cyclic potentiodynamic polarization curves were measured at a scan rate 1 mV/s from the open circuit potential (OCP) until the current density reached 5 mA.cm⁻², at which point the scanning direction was then reversed.

The specimens for the electrochemical tests (cyclic polarization, CPT, and EIS) were extracted from the samples of each of the steels. Samples were properly prepared before each electrochemical test.

To determine the critical pitting temperature (CPT), a constant potential of 750 mV_{Ag/AgCl} was applied. For the CPT test, a saline solution of 3.5 wt% NaCl was heated at a rate of approximately 1 °C/min. During the tests, current densities and corresponding temperatures were obtained respectively from PSTrace 4.2 software and the readings on the digital thermometer immersed in the solution. The tests were performed until the current density reached approximately 200 µA/cm². The pits formed in the samples after potentiodynamic polarization tests and CPT were observed using a scanning electron microscope (SEM) TESCAN, VEGA3 model.

3. RESULTS AND DISCUSSION

3.1 Cyclic polarization analysis

Figure 1 shows the cyclic polarization curves of the UNS S31803 and UNS S32304steels tested in 3.5 wt% NaCl solution. Electrochemical parameters obtained in the tests are shown in Table 2.

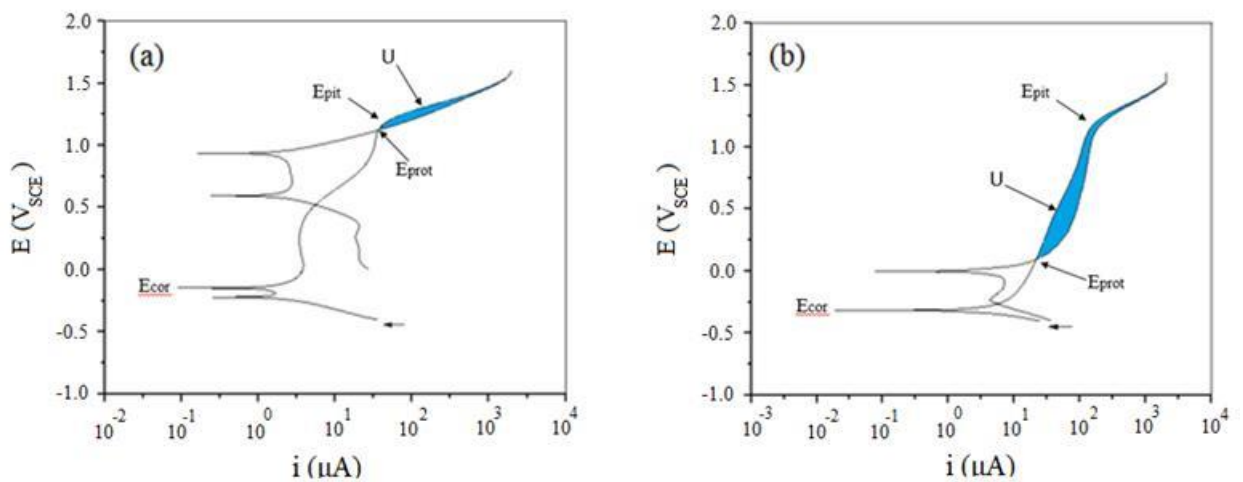


Figure 1: Cyclic polarization curves: (a) UNS S31803; (b) UNS S32304. (3.5 wt% NaCl; 25°C; 0.167 mV/s).

Table 2: Electrochemical parameters of UNS S31803 and UNS S32304 steels. (3.5 wt% NaCl; 25°C; 0.167 mV/s).

SAMPLES	E _{cor} (V _{ECS})	E _{pit} (V _{ECS})	E _{prot} (V _{ECS})	(E _{pit} - E _{prot}) (V _{ECS})	U (C/cm ²)
UNS S31803	-0.16 ± 0.04	1.21 ± 0.03	1.12 ± 0.05	0.09 ± 0.03	1.20
UNS S32304	-0.32 ± 0.03	1.16 ± 0.03	0.10 ± 0.06	1.06 ± 0.03	3.23

As can be seen from the curves shown in Figure 1, the corrosion potential (E_{corr}) indicates the limit value below which the metal dissolution rate is low, due to the predominance of cathodic reactions. Above the E_{corr} there is reversal of the current and, from that, starts the anodic region of the polarization curve. Initially, the anode region is considered active. In this region, anodic dissolution of the metal and oxidation of the solution compounds occur. The stainless steel anode active region is bounded by a potential value, above which, even with the increase of the potential, the current remains more or less constant. This is the passive region that is characterized by low corrosion rate [12].

The polarization curves of both steels have the typical behavior of materials that exhibit passivation. From the E_{corr} the current increases in the active region and tends to stabilize when the passivation occurs. At higher values of applied potential, transpassivation occurs where normally there is the growing of pits or passive layer degradation [15].

As can be seen in Figure 2, the UNS S32304 steel showed lower E_{corr} than the UNS S31803 steel, showing its greater susceptibility to corrosion. Although the E_{pit} of the two steels did not present a significant difference, the repassivation potential (E_{prot}) of the UNS S31803 steel was higher than that of the UNS S32304 steel. This means that UNS S31803 steel can restore the passive layer inside the pits more easily than UNS S32304 steel.

The bounded areas of the steel repassivation hysteresis shown in Figure 1 (Electrical work “U”) correspond to the energy needed for repassivation of the pits formed. The higher the electrical work (U) implies higher repassivation resistance of the pits [16]. The smallest difference between E_{pit} and E_{prot} of the steel implies higher capacity to recover the passive layer in the pit [9]. Thus, according to the results obtained, UNS S31803 steel presents more resistance to pitting compared to UNS S32304 steel.

As can be seen in Table 2, the UNS S32304 steel showed a difference ($E_{\text{pit}} - E_{\text{prot}}$) about 11.8 times greater than the UNS S31803 steel. Larger pits in the UNS S32304 steel, compared with the UNS S31803 steel, can be observed in Figure 2. It can be seen that even the pit density formed in the UNS S32304 steel was also higher compared to UNS S31803 steel.

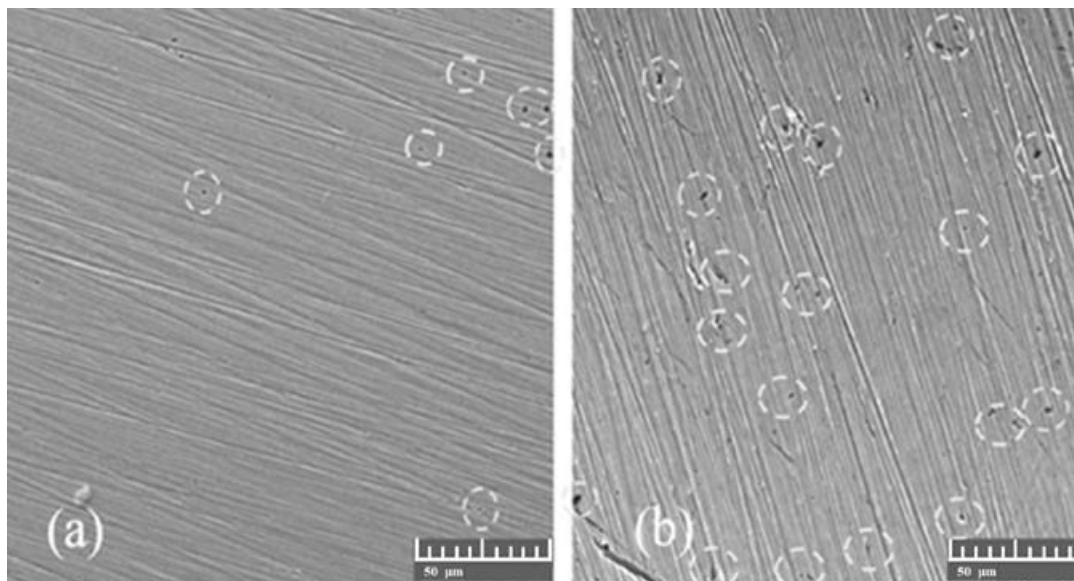


Figure 2: SEM pits on the surface specimens after potentiodynamic polarization tests: (a) UNS S31803; (b) UNS S32304.

The best results related to the passivation potential (E_{prot}) and electrical work (U) obtained by the UNS S31803 steel, compared with the UNS S32304 steel, can be attributed to the presence of molybdenum in the first steel. Molybdenum contributes to the formation, homogenization, and stability of the passive layer in duplex stainless steels [17]. According to the Pitting Resistance Number (PREN), UNS S31803 steel (PREN = 34.8) presents greater resistance to pitting formation than UNS S32304 steel (PREN = 26.1). PREN can be calculated from the chemical composition of steel using Equation 1 [18]. In addition to the molybdenum, the presence of chromium, nickel, and nitrogen also contribute to stabilizing the passive layer, retarding its dissolution and improving its reconstitution capacity [10, 19-20].

$$\text{PREN} = \% \text{Cr} + 3.3(\% \text{Mo}) + 16(\% \text{N}) \quad (1)$$

The chromium equivalent (Cr_{eq}) and nickel equivalent (Ni_{eq}), related to the steel chemical composition, can also predict the susceptibility of pitting corrosion of stainless steels. The pitting corrosion resistance decreases with the increase of $\text{Cr}_{\text{eq}}/\text{Ni}_{\text{eq}}$. Cr_{eq} and Ni_{eq} can be calculated by Equations 2 and 3, respectively, proposed by the Welding Research Council (WRC) 1992 diagram [21].

$$\text{Cr}_{\text{eq}} = \% \text{Cr} + \% \text{Mo} + 0.7\% \text{Nb} \quad (2)$$

$$\text{Ni}_{\text{eq}} = \% \text{Ni} + 35\% \text{C} + 20\% \text{N} + 0.25\% \text{Cu} \quad (3)$$

Based on the $\text{Cr}_{\text{eq}}/\text{Ni}_{\text{eq}}$ relationship, it can be predicted that UNS S31803 steel ($\text{Cr}_{\text{eq}}/\text{Ni}_{\text{eq}} = 2.59$) appears more resistant to pitting corrosion than UNS S32304 steel ($\text{Cr}_{\text{eq}}/\text{Ni}_{\text{eq}} = 2.86$), according to the results of the potentiodynamic polarization and CPT tests. In relation to the presence of molybdenum, Deng et al. [22] show that, at the annealing temperature of 1060°C, UNS S31803 steel presents higher molybdenum content in the ferritic phase than in the austenitic phase. Thus, the ferritic phase becomes more susceptible to pitting at this temperature.

Figure 3 shows the average curves of current densities as a function of corresponding temperatures of the solution during the application of potential on CPT tests.

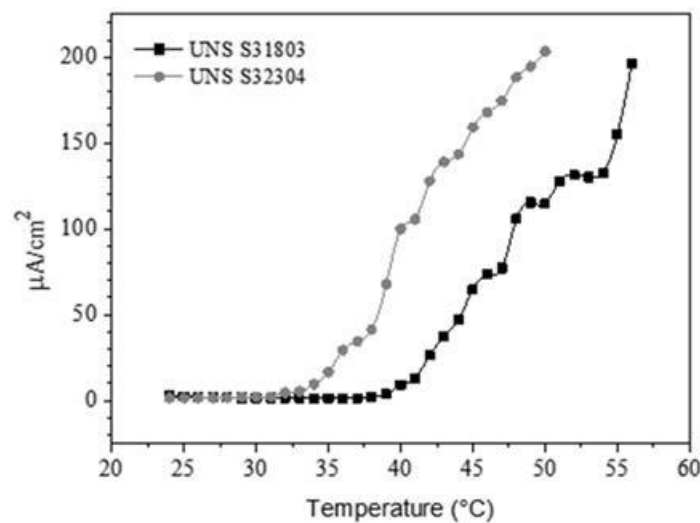


Figure 3: Current density variation on the UNS S32304 and UNS S31803 as function of the temperature during the CPT tests. (3.5 wt% NaCl; 750 mV_{SCE}; 1°C/min).

The critical pitting temperature (CPT) was considered the temperature at which the current density reached 100 µA/cm² [22,23]. As can be seen in Figure 4, the UNS S31803 steel showed a higher CPT compared to the UNS S32304 steel, confirming its superiority over the resistance to pitting formation in 3.5 wt.% NaCl. Higher PREN and $\text{Cr}_{\text{eq}}/\text{Ni}_{\text{eq}}$ of the UNS S31803 steel contributed to its greater CPT.

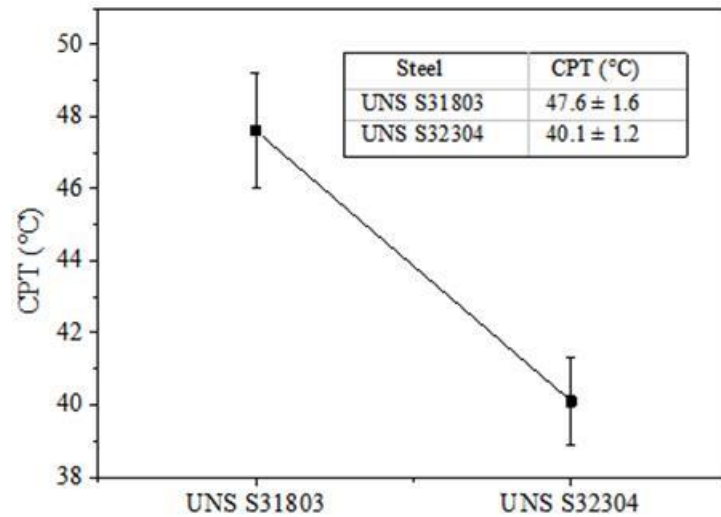


Figure 4: CPT of UNS S31803 and UNS S32304 steels. (3.5 wt% NaCl; 750 mV_{SCE}; 1°C/min).

Increasing the temperature increases the susceptibility to pitting corrosion due to destabilization of the passive layer. Corrosion is a process thermally activated [22, 24]. Figure 5 shows the higher pit density on the surface of the UNS S32304 steel in comparison with the UNS S31803 steel, formed during CPT tests. The UNS S32304 steel presented greater sensitivity to pit formation with increasing temperature. This behavior of higher pitting density in UNS S32304 steel can be attributed to the lower content of molybdenum in its composition compared to UNS S31803 steel.

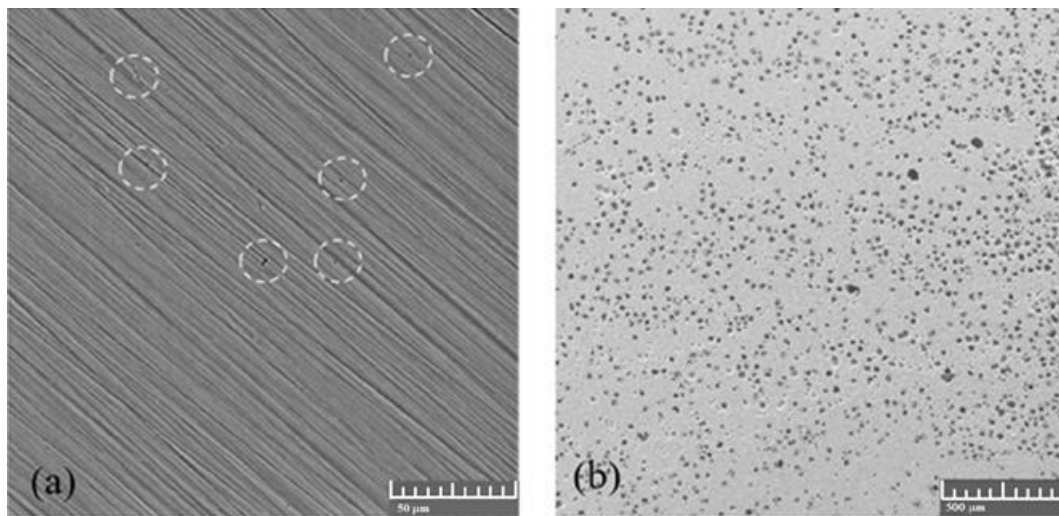


Figure 5: SEM pits on the surface specimens after CPT tests: (a) UNS S31803; (b) UNS S32304.

3.2 EIS analysis

The EIS was utilized to explore the corrosion behavior of UNS S31803 and UNS S32304 duplex stainless steels on the electrochemical properties of the passive film in 3.5 wt% NaCl solution. Nyquist and Bode phase angle curves obtained in the 3.5 wt% NaCl solution of the UNS S31803 and UNS S32304 steels are shown in Figure 6 (a, b).

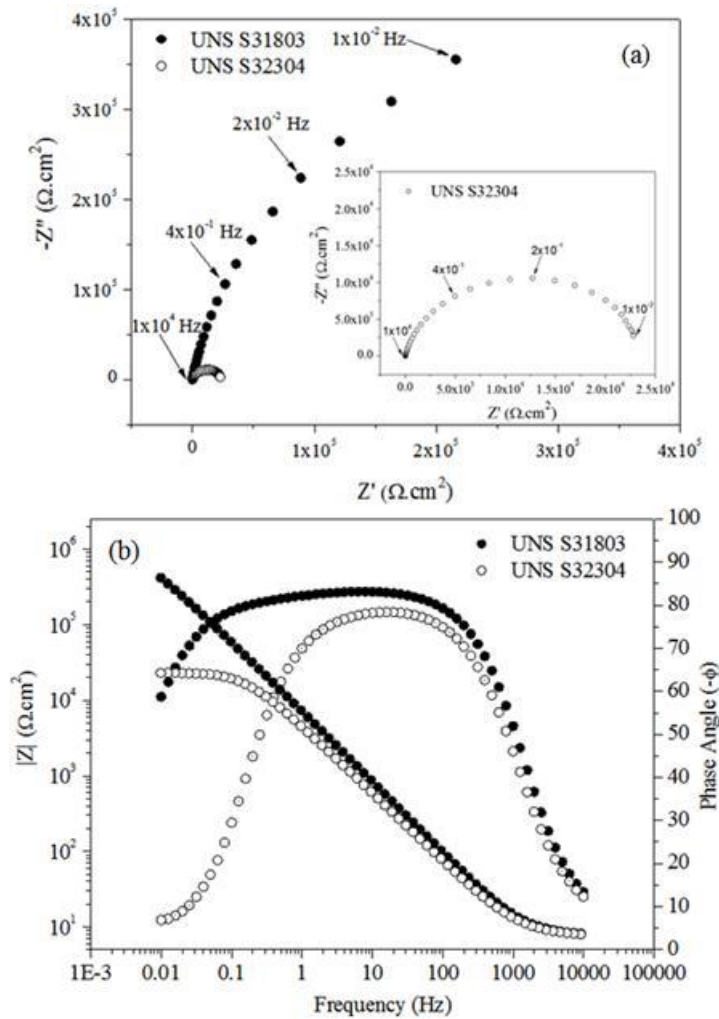


Figure 6: (a) Nyquist diagrams and (b) Bode diagrams of impedance modulus and phase angle for the UNS S31803 and UNS S32304 steels. (3.5 wt% NaCl; 25°C).

The larger diameters of the capacitive semi-circles indicated a higher corrosion resistance of the passive film in 3.5 wt% NaCl solution (Figure 6a). Figure 6b shows Bode curves of the UNS S31803 and UNS S32304 steels. There are many equivalent circuit models for fitting the impedance spectra results [25].

The equivalent circuits in Figure 7(a, b) were proposed as a model for fitting the EIS results. As shown in the equivalent circuits, an R_s is connected in series with two R-CPE (constant phase element) elements in parallel, with two time constants [26]. The CPE was used in the fitting procedure because of the non-ideal capacitance response of the interface [27]. In these equivalent circuit models, R_s is the electrolyte resistance. R_1 and R_2 stand for the resistance of the passive film and charge transfer resistance, respectively. CPE1 and CPE2 are the capacitance of the passive film and double layer capacitance. The detailed fitting parameters of the obtained EIS results are listed in Table 3.

The greater values of film resistance (R_1) and charge transfer process (R_2), and the lower value of CPE1 were obtained for the UNS S31803 steel, suggesting its higher protective ability of the passive film due to the fewer defects in it. The polarization resistance (R_p), defined as the sum of R_1 and R_2 , is associated with the corrosive process between the metal and the solution, which occurs through the protective passive film. It was observed that the UNS S31803 steel showed a higher polarization resistance ($R_p = 10.79 \times 10^5 \pm 6.46 \times 10^3 \Omega \cdot \text{cm}^2$) than the UNS S32304 steel ($R_p = 2.37 \times 10^4 \pm 3.66 \times 10^2 \Omega \cdot \text{cm}^2$). The EIS equivalent circuits shown in Figure 7 indicate that the corrosion behavior of the two steels is compatible with the following models: (a) the equivalent circuit fitted to the EIS data for the UNS S31803 steel was associated with a corrosion process occurring through pores in the oxide film (Figure 7a); (b) the equivalent circuit fitted to the EIS data of the UNS S32304 steel to the corrosion process occurred at the metal/film interface (Figure 7b). The results of cyclic polarization and CPT tests are compatible with the models proposed by the

EIS equivalent circuits. Also, the cyclic polarization and CPT test results showed that the UNS S31803 steel presented higher corrosion resistance than the UNS S32304 steel in the studied condition.

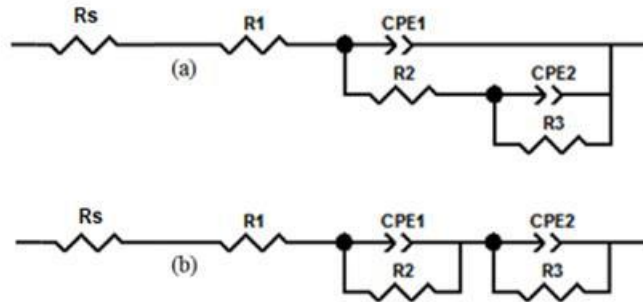


Figure 7: Equivalent circuits for the corrosion behavior: (a) UNS S31803: (b) UNS S32304.

Table 3: Electrochemical parameters obtained from impedance curves in 3.5 wt% NaCl for the UNS S31803 and UNS S32304 steels.

SAMPLES	R1/ $\Omega.cm^2$	CPE1/ $F.cm^2$	n1	R2/ $\Omega.cm^2$	CPE2/ $F.cm^2$	n2	R3/ $\Omega.cm^2$	χ^2
UNS S31803	7.94 ± 0.03	2.47×10^{-5} $\pm 1.25 \times 10^{-7}$	0.927 $\pm 8.49 \times 10^{-4}$	3.52×10^5 $\pm 8.65 \times 10^2$	3.80×10^{-6} $\pm 1.17 \times 10^{-7}$	0.768 ± 0.073	7.27×10^5 $\pm 1.00 \times 10^4$	6.08×10^{-4}
UNS S32304	7.61 ± 0.04	3.74×10^{-4} $\pm 1.51 \times 10^{-6}$	0.771 ± 0.018	7.78×10^2 $\pm 5.10 \times 10^1$	4.15×10^{-5} $\pm 1.56 \times 10^{-6}$	0.929 $\pm 8.96 \times 10^{-3}$	2.29×10^4 $\pm 5.68 \times 10^2$	4.98×10^{-4}

Comparing the two stainless steels in 3.5 wt% NaCl solution, the UNS S31803 steel, which showed the highest PREN number and highest content of nickel and molybdenum, showed a higher polarization resistance than the UNS S32304 steel. This suggests that UNS S31803 steels are more resistant to corrosion in 3.5 wt% NaCl solution; i.e., the passive film is more protective. The content of Ni and Mo extends the passive region and strengthens the passive layers of the samples improving corrosion resistance [28].

4. CONCLUSIONS

- The cyclic polarization results of the UNS S31803 and UNS S32304 steels in a chloride environment showed similar values of pitting potential for both steels but the UNS S31803 steel showed a higher protection potential, and lower values of passivation current density and hysteresis area than the UNS S32304 steel. The UNS S31803 steel showed better repassivation ability of the passive layer than the UNS S32304 steel.
- The corrosion mechanism evaluated by EIS results in a saline medium was different for the duplex and lean duplex steel.
- The corrosion mechanism of the UNS S31803 showed two time constants and was performed through the pores in the layer.
- The corrosion mechanism of the UNS S32304 involved two time constants relating to the passive layer and the corrosion process occurring at the metal/oxide interface.
- The critical pitting temperature was higher for the UNS S31803 than the UNS S32304 steel.

5. ACKNOWLEDGEMENTS

The authors would like to acknowledge the GPESE (Grupo de Pesquisa em Sistemas de Exaustão) and Universidade Federal de Itajubá, Campus Itabira - Brazil for providing the equipment and technical support for experiments. The authors also thank APERAM South America, Timóteo City, Minas Gerais State, Brazil, for the supplied specimens. This study was funded by Conselho Nacional de Desenvolvimento Científico e Tecnológico, CNPq, (grantnumber 303735/2015-5), and CAPES (Coordenação de Aperfeiçoamento de Pessoal de Nível Superior). The authors declare that they have no conflict of interest.

6. BIBLIOGRAPHY

- [1] CRAMER, S. D., COVINO, B. S.; MOOSBRUGGER, C. *Corrosion: Fundamentals, Testing, and Protection*, ASM Handbook, v. 13A, ASM International, 2003.
- [2] PANNONI, F. D., *Coletânea do Uso de Aço: Princípios da Proteção de Estrutura Metálicas em Situação de Corrosão e Incêndio*, 5 ed., Gerda Aço Minas, 2011.
- [3] LIPPOLD, J. C., KISER, S. D., DUPONT, J. N., *Welding metallurgy and weldability of nickel-base alloys*, John Wiley & Sons, 2014.
- [4] CICEK, V., *Corrosion Engineering and Cathodic Protection Handbook: With an Extensive Question and Answer Section*, John Wiley & Sons, 2017.
- [5] MÉSZÁROS, I., SZABÓ, P. J., “Complex magnetic and microstructural investigation of duplex stainless steel”, *NDT & E International*, v. 38, pp. 517-521, 2005. DOI: 10.1016/j.ndteint.2004.12.007
- [6] GUNN, R. N., *Duplex stainless steels: microstructure, properties and applications*, Cambridge England, Abington Publishing, 1997.
- [7] POHJANNE, P., CARPÉNA, L., HAKKARAINEND, T., *et al.*, “Method to predict pitting corrosion of stainless steels in evaporative conditions”, *Journal of Construction Steel Research*. v. 64, pp. 1325-1331, 2008. DOI: 10.1016/j.jcsr.2008.07.001
- [8] TOTTEN, G. E., *Steel heat treatment: metallurgy and technologies*, Taylor & Francis Ltda, 2007.
- [9] LEE, Shuo-Jen, LAI, Jian-Jang, HUANG, Ching-Han., “Stainless steel bipolar plates”, *Journal of Power Sources*, v. 145, pp. 362-368, 2005. DOI: 10.1016/j.jpowsour.2005.01.082
- [10] CHENG, X., WANG, Y., LI, X., *et al.*, “Interaction between austenite-ferrite phases on passive performance of 2205 duplex stainless steel”, *Journal of Materials Science & Technology*, v. 34, n. 11, pp. 2140-2148, 2018. DOI: 10.1016/j.jmst.2018.02.020
- [11] ALVAREZ-ARMAS, I., “Duplex stainless: brief history and some recent alloys” *Recent Patents on Mechanical Engineering*, v. 1, n. 1, pp. 51-57, 2008.
- [12] MÉLO, E. B. D., MAGNABOSCO, R., MOURA NETO, C. D., “Influence of the microstructure on the degree of sensitization of a duplex stainless steel UNS S31803 aged at 650°C”. *Materials Research*, v.16, n.6, pp. 1336-1343, 2013. DOI: 10.1590/S1516-14392013005000125
- [13] KINA, A. Y., SOUZA, V. M., TAVARES, S. S. M., *et al.*, “Microstructure and intergranular corrosion resistance evaluation of AISI 304 steel for high temperature service”, *Materials characterization*, v. 59, n. 5, pp. 651-655, 2008. DOI: 10.1016/j.matchar.2007.04.004
- [14] Anonymous (2014), G5-14e1, *Standard Reference Test Method for Making Potentiodynamic Anodic Polarization Measurements*.
- [15] ALAMERI, M., YI, Y., CHO, P., *et al.*, “Critical conditions for pit initiation and growth of austenitic stainless steels”, *Corrosion Science*, v. 92, pp. 209-216, 2015. DOI: 10.1016/j.corsci.2014.12.006
- [16] GIORDANI, E. J., FERREIRA, I., BALANCIN, O., “Propriedades mecânicas e de corrosão de dois aços inoxidáveis austeníticos utilizados na fabricação de implantes ortopédicos”, *REM: Revista da Escola de Minas*, v. 60, n.1, 2007. DOI: 10.1590/S0370-44672007000100009
- [17] POTGIETER, J. H., “Influence of σ phase on general and pitting corrosion resistance of SAF 2205 duplex stainless steels”, *Corrosion Engineering, Science and Technology*, v. 27, pp. 219-223, 1992. DOI: 10.1179/000705992798268530
- [18] ZHANG, Z., JING, H., XU, L., *et al.*, “Effect of post-weld heat treatment on microstructure evolution and pitting corrosion resistance of electron beam-welded duplex stainless steel”, *Corrosion Science*, v. 141, pp. 30-45, 2018. DOI: 10.1016/j.corsci.2012.04.047
- [19] KANG, D. H., LEE, H. W., “Study of the correlation between pitting corrosion and the component ratio

- of the dual phase in duplex stainless steel welds”, *Corrosion Science*, v. 74, pp. 396-407, 2013. DOI: 10.1016/j.corsci.2013.04.033
- [20] ROBERGE, P., *Handbook of Corrosion Engineering*, McGraw Hill Professional. 2012.
- [21] JIANG, Y., TAN, H., WANG, Z., *et al.*, “Influence of Creq/Nieq on pitting corrosion resistance and mechanical properties of UNS S32304 duplex stainless steel welded joints”, *Corrosion Science*, v.70, pp. 252-259, 2013. DOI: 10.1016/j.corsci.2013.01.037
- [22] DENG, B., WANG, Z., JIANG, Y., *et al.*, “Effect of thermal cycles on the corrosion and mechanical properties of UNS S31803 duplex stainless steel”, *Corrosion Science*, v. 51, pp. 2969-2975, 2009. DOI: 10.1016/j.corsci.2009.08.015
- [23] SOLTIS, J., “Passivity breakdown, pit initiation and propagation of pits in metallic materials–review”, *Corrosion Science*, v. 90, pp. 5-22, 2015. DOI: 10.1016/j.corsci.2014.10.006
- [24] SILVERMAN, D. C., *Practical Corrosion Prediction Using Electrochemical Techniques*, in *Uhlig's Corrosion Handbook*, 3 ed, New York, John Wiley & Sons, Inc., 2011.
- [25] KOCIJAN, A., MERL, D. K., JENKO, M., “The corrosion behaviour of austenitic and duplex stainless steels in artificial saliva with the addition of fluoride”, *Corrosion Science*, v. 53, pp. 776-783, 2011. DOI: 10.1016/j.corsci.2010.11.010
- [26] FREIRE, L., CARMEZIM, M. J., FERREIRA, M. G. S., *et al.*, “The passive behaviour of AISI 316 in alkaline media and the effect of pH: A combined electrochemical and analytical study”. *Electrochimica Acta*, v. 56, pp. 5280-5289, 2011. DOI: 10.1016/j.electacta.2009.10.026
- [27] WALLINDER, D., PAN, J., LEYGRAF, C., *et al.*, “EIS and XPS study of surface modification of 316LVM stainless steel after passivation”, *Corrosion Science*, v. 41, pp. 275-289, 1998. DOI: 10.1016/S0010-938X(98)00122-X
- [28] BLASCO-TAMARIT, E., IGUAL-MUNÓZ, A., ANTÓN J. G., *et al.*, “Effect of aqueous LiBr solutions on the corrosion resistance and galvanic corrosion of an austenitic stainless steel in its welded and non-welded condition”, *Corrosion Science*, v. 48, n.4, pp. 863-886, 2006. DOI: 10.1016/j.corsci.2005.02.028

ORCID

José Carlos de Lacerda	http://orcid.org/0000-0001-7753-1713
Ricardo Luiz Perez Teixeira	https://orcid.org/0000-0003-2641-4036
Rafaella Maria Ribeiro de Souza	https://orcid.org/0000-0001-7405-3787
Renata Braga Soares	https://orcid.org/0000-0002-3625-4307
Vanessa de Freitas Cunha Lins	https://orcid.org/0000-0002-6357-9553